Sensor Applications

Indoor Visible Light Positioning for A Single Partially Visible LED

Srivathsan Chakaravarthi Narasimman* and Arokiaswami Alphones**
School of Electrical and Electronics Engineering,Nanyang Technological University,Singapore
** Graduate Student Member, IEEE*
*** Senior Member, IEEE*

Abstract—With the IEEE 802.11bb standard being adopted to incorporate light communication, research interest in visible light positioning (VLP) has increased. While several VLP techniques have seen success using complementary metal oxide semiconductor (CMOS) sensors for a single LED, in most cases the field of view (FoV) of a front camera on a smartphone is much smaller than the rear camera and lights are placed sparsely in offices since their primary objective is illumination. Hence, during indoor navigation the front camera is bound to encounter far more partial images of the light than complete images. The proposed technique seeks to solve this problem by performing positioning on images where only two corners of a square light are in the FoV. While most offices have square or rectangular panel lights, we have chosen to use square lights owing to the added difficulty in positioning arising from all sides being equal in length. We detect the corners of the light from an image and order them based on inertial measurement unit (IMU) readings from smartphones to perform structure-based positioning. The proposed technique achieved 2.27cm average 3D positioning error on a partial light image dataset captured at two different heights.

Index Terms—Visible light positioning, single partially visible LED, occlusion, camera, computer vision, indoor localization

I. INTRODUCTION

The VLP techniques use either photo detectors (PDs) or cameras as receivers. While photo detectors are capable of high data rate visible light communication (VLC) when compared to cameras, they are worse than cameras at localisation. The cheap CMOS sensors available on smartphones are an obvious choice for techniques that seek practical implementation of VLP in extant spaces. The location of the transmitter must be identified after which the location of the receiver with respect to the transmitter can be identified. The transmitter identification problem in this case is an indoor positioning problem using smartphones, which has been explored for several decades. Radio fingerprinting techniques have been shown to provide accurate floor and building detection across several datasets[1], [2], and magnetic field strength has been shown to achieve sub meter accuracy[3], [4] which is close enough to identify the transmitter location owing to the sparse distribution of indoor lights. VLC has also been employed with cameras for light identification[5]–[7] by encoding unique codes in lights acting as beacons. Owing to the many well established options for transmitter identification, this letter will explore the relative pose and position identification assuming the transmitter location is known.

The camera-based single LED positioning problem has been explored extensively. In the case of circular panel lights, circle projection was used to estimate position and a red marker on the light was used to identify orientation in [6] while geometric features from consecutive frames were used to improve positioning accuracy in [5] and plane intersection with line scheme was used to facilitate positioning in [8] . Ellipse fitting was used for positioning and projective geometry was using to calibrate an IMU in [9]. In the case of rectangular panel lights, corners are widely used for positioning. Corners were used with the perspective n point (PnP) approach in [10], with random forest regression in [11], with the perspective n line (PnL) approach in [7]. Since at least three known point correspondences are needed in these approaches, they have yet to be applied for partially visible lights in images.

The proposed technique seeks to address this gap by using two known points to estimate two more points on parallel sides of the rectangular panel light. These estimated points allow the use of the PnL approach. While the fusion of inertial sensor information for the identification of azimuthal angle is well explored with deep learning[12] and graph optimisation[13], it produces erroneous results due to uncalibrated IMU on smartphones. The proposed technique seeks to identify the general direction in which the phone is pointing when the image is taken reducing the accuracy requirement of the IMU.

The main contributions of this work are listed as follows

- A novel single LED VLP technique that outperforms the current state of the art technique.
- The first VLP technique to detect pose and position when only two corners of a four corner LED are visible.

II. METHODOLOGY

A. Problem Description

The layout of a camera-based single LED VLP problem is shown in Fig. 1(a), where a square LED panel with its corners marked $P1$ to $P4$ is in the ceiling of a room. The axes of the world coordinate system (WCS) are marked with subscript W and the axes of the phone coordinate system (PCS) are marked with subscript p. The axes marked N, E and U point towards the magnetic north, geographical east and up directions respectively. The magnetometer on the phone will provide the orientation of N with respect to the PCS Y_p axis. The height of the camera from the transmitter is marked h_t. An image of an LED panel from the camera on the phone is shown in Fig. 1(b), where the pixel coordinate system (PiCS) with its origin in the top left of the image.

The image coordinate system (ICS) shown in Fig. 1(c), moves the origin O_i to the centre of the image and converts the units from pixels

Corresponding author: A. Alphones (e-mail: EAlphones@ntu.edu.sg).

Digital Object Identifier 10.1109/LSENS.2017.0000000

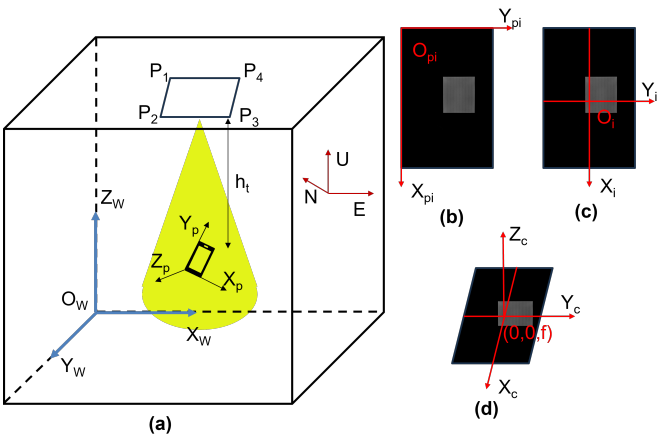

Fig. 1. Coordinate system layout.

to meters. The centre of the image is subtracted from the coordinate of a point in PiCS and multiplied by the size of a pixel in meters to get corresponding ICS coordinates. The camera coordinate system (CCS) places the image plane in 3D space at focal length f from the CMOS sensor as shown in Fig. 1(d). The rotation and translation of CCS with respect to the WCS provides the pose and position of the receiver with respect to the transmitter. There are two parts to the positioning problem, identifying the location of the light and estimating the relative position of the receiver. This letter will focus on the second part while the light location and its orientation with respect to the magnetic north are assumed to be known accurately.

B. Experimental Setup

Images were captured on a Redmi Note 9 Pro smartphone placed on a tripod as shown in Fig. 2(a), with the position being tracked using a 1.2m X 1.2m grid of tape on the ground, where each cell was 40 cm apart, and the pose being tracked using an inclinometer, for pitch and roll, and a compass for azimuth. Five images were captured at each location on the grid with the phone facing the door and away from it, along with IMU readings using sensors on board the smartphone. One set of images was captured with different poses always ensuring all four corners of the light were within the FoV of the camera and another set was captured such that only two of the LED corners were in the FoV.

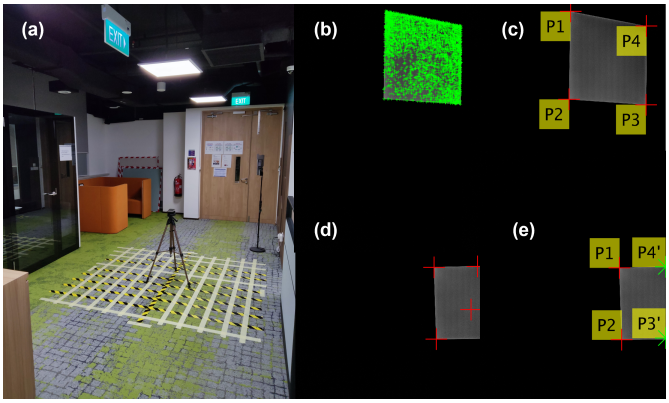

Fig. 2. (a) Experimental Setup (b) all detected corners (c) strongest 4 labelled corners (d) incorrect occluded light corners (e) corrected labelled corners.

The images were also captured at four different heights from the transmitter ranging from 120cm to 156cm in 12cm increments. Thus 640 images comprising of 5 images with different poses at 16 grid locations facing two different general directions at four heights was captured for the complete light dataset. The general direction was found to have minimal impact on the positioning accuracy, so the partial light dataset was captured in only one direction with 120 images comprising of 5 images with different poses at only the outer 12 grid locations at 120cm and 156cm from the light. These images, the ground truth pose and position along with the known light location and orientation were used for localization.

C. Corner Detection and Ordering

Structure based VLP techniques leverage known points in WCS and CCS. Since the images were captured at 68 microsecond exposure time with 100 ISO only the light was visible with a black background. This was done to facilitate VLC where the exposure time determines the maximum data rate and to ensure feature detection from the image is easier. We detected the corners using the Shi-Tomasi algorithm[14] which uses the minimum Eigen value as a scoring function. The detected corners are shown in green in the Fig. 2(b) where multiple points are flagged apart from the actual corners of the panel light. The four strongest points, with the highest scoring function among the detected corners are shown in Fig. 2(c). Since a square LED panel is used, there were four possible orders for the points depending on the orientation of the phone. The points were sorted based on the orientation from the IMU which was then compared with the known orientation of the light to detect the general direction in which the phone was pointing with respect to the light. The strongest four corners were not always the four corner points in the partial light dataset as shown in Fig. 1(d). In this case, we used the two strongest corners as the known corners. Depending on the axis along which the difference between the known corner points was highest, all detected corners along the axis of minor deviation between known corners were filtered and the furthest among these points from the known corners were chosen as the estimated corners labelled $P3'$ and $P4'$ in Fig. 1(e).

D. Positioning Technique

Once the corners are detected in the PiCS, the CCS coordinates of the same can be obtained from the pixel size and focal length. The corner points in the WCS are calculated from the known size of the light. To obtain the relationship between WCS and CCS, coordinates of the same points in both the systems are needed. The coordinates of the light corners in CCS are known to be a scalar multiple of the image corner coordinates in CCS[15] as shown below

$$P_i^C = \lambda_i \times p_i^C, \qquad i = 1, 2, 3, 4 \tag{1}$$

where λ_i is the scalar multiple for each corner point. To solve for these four unknowns the known sides of the light were used in [15], which works only when the entire light is visible. When the light is partially visible, the Euclidean distance between known points of the panel light will provide one equation as follows

$$\|P_i^C - P_j^C\| = d_{i,j} \tag{2}$$

where P_i^C and P_j^C are the two visible corner points in the CCS and $d_{i,j}$ is the distance between corner points which will be the same here since the light is square. We also know that the sides

are perpendicular, so even if the exact corner points are not known estimated corner points in the same direction as the actual corner are obtained as shown in Fig. 2(e). The dot product of these sides will then be zero, as follows

$$(P_i^C - P_j^C) \cdot (P_i^C - P_{k'}^C) = 0 \tag{3}$$

$$(P_i^C - P_j^C) \cdot (P_j^C - P_{m'}^C) = 0 \tag{4}$$

where $P_{k'}^C$ and $P_{m'}^C$ are the estimated corner points. We know that all four points are coplanar, which can be defined as follows

$$\{(P_i^C - P_j^C) \times (P_i^C - P_{k'}^C)\} \cdot (P_j^C - P_{m'}^C) = 0 \tag{5}$$

Now we have four equations in four unknowns which can be solved to find the scalar constants λ_i for the four points using which the corner points in the CCS can be obtained. The relationship between CCS and WCS is shown below

$$P_i^W = R_C^W \cdot p_i^C + \theta_C^W, \qquad i = 1, 2, 3, 4 \tag{6}$$

where R_C^W is the rotation matrix which provides the pose and θ_C^W is the translation vector which provides the position. We performed positioning by solving this equation using Levenberg-Marquardt optimisation technique.

III. RESULTS AND DISCUSSION

Some of the best camera-based single panel VLP systems are shown in table 2, where LED refers to the panel light shape and the full and part columns refer to fully and partially visible lights. Among the square panel techniques [11] estimated only the position and not the pose. Since [7] performed the best it was chosen as the state of the art (SOTA) technique for comparison with the proposed technique. The proposed technique was the only technique capable of positioning with two corners and also the most accurate VLP technique for fully visible lights.

A. Orientation Identification

TABLE 1. Azimuthal error results

Height(cm)	120	132	144	156
Angle error(degrees)	10.85	15.63	18.86	18.74

The orientation data from the IMU on the phone is recorded along with all the images. Since the light is a square, identification of the side on the top of the image is essential for correct labelling of corner points. As there are four equal sides, if the error of azimuth detection is less than 45° the general direction in which the phone Y_P axis is pointing can be identified accurately. The error between the magnetic north from the IMU and the known magnetic north direction in degrees is shown in table 1, where the average absolute error for all the images at different heights from the transmitter are shown. The average error is less than half of the forty five degree threshold ensuring accurate orientation detection and hence accurate corner labelling.

B. Full LED Detection

The proposed positioning technique was applied to the full light dataset and the results were compared with the SOTA V-P4L algorithm[7]. The SOTA proposes operating the four corner LEDs of a rectangular panel light individually to beam a unique code from each of them facilitating accurate corner detection and labelling. Since this is not possible on commercial off the shelf (COTS) panel lights, they have used four different LED lights to mark the corners of a rectangular panel light. We have employed the V-P4L algorithm with the corners detected and labelled using our proposed technique. The mean 3D positioning error is the mean Euclidean distance between the actual location and the predicted location. The cumulative distribution function (CDF) of the results from the proposed technique and the SOTA are marked as such in Fig. 3, where the title of each individual plot is the distance between the transmitter and the receiver. The proposed technique performs better than the SOTA at all four heights and the maximum error reduces as the distance between the transmitter and receiver decreases.

TABLE 2. Comparison of camera-based single LED VLP systems

Ref.	***Method***	***LED***	***3D error (cm)***		***Area (m^2)***	***Height (m)***
			Full	**Part**		
[5]	circle features	○	7	-	1.8X1.8	1-1.4
[6]	circle projection	○	15.15	-	3X3	1.5-2
[11]	random forest	□	4	-	1.2X1.2	1.23-1.66
[10]	corner PnP	□	4.6	-	1X1	1-2
[7]	corner PnL	□	2.73	-	0.5X0.5	1.48
This work	est. corner PnL	□	0.9	2.27	1.2X1.2	1.2-1.56

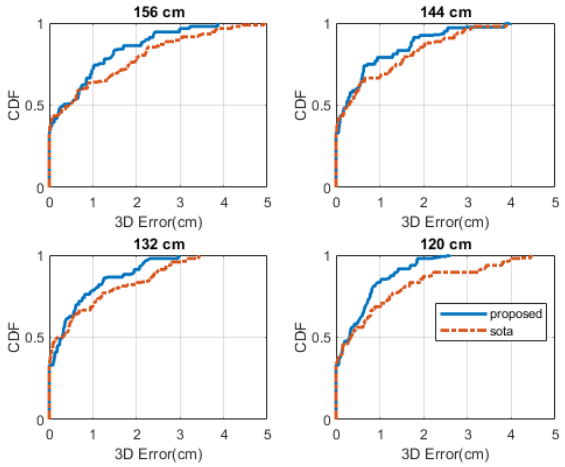

Fig. 3. CDF of 3D mean positioning errors at different heights from transmitter.

The pose error is the mean absolute difference between the estimated angle and the ground truth along the three axes. The angle error about all three axes for both the proposed technique and the SOTA is shown in Fig. 4, where they are plotted as a function of the distance between the transmitter and receiver. The SOTA performs marginally better or the same as the proposed technique for the x and y axes but the z axis, which is the azimuth, sees a drastic drop is accuracy from the SOTA compared to the proposed technique. There was no clear correlation between the angle errors and the height from the transmitter for either the SOTA or the proposed technique.

C. Partially Visible LED Detection

The results of the proposed technique on the partial light dataset are shown in Fig. 5, where the mean 3D positioning error at each grid location is reported for the two different heights from the transmitter. The error increases with the distance between transmitter and receiver. The error at 156cm is either equal or higher than 120cm at all the

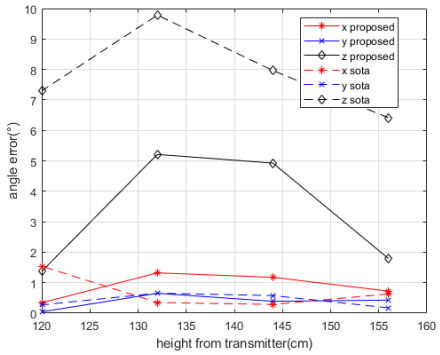

Fig. 4. Angle errors of the proposed and SOTA techniques at different heights from transmitter.

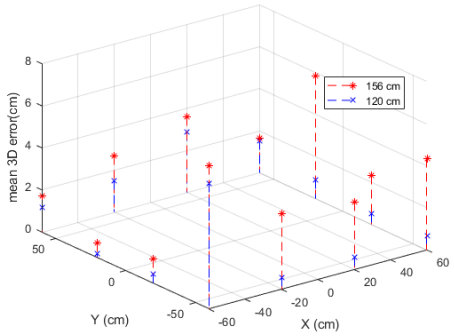

Fig. 5. Positioning errors of the proposed technique on partially visible lights.

twelve grid locations. Though the SOTA estimates pose and position when three corners are visible, there are no other techniques to the best of our knowledge which have performed visible light positioning when two corners are visible. Hence the results are compared with the full light dataset positioning results in the table 3,where the # of corners refers to the number of corners of the light visible in the image. While sub 6cm accuracy was achieved for the partial light

TABLE 3. Positioning error results

# of corners	***Height(cm)***	***3D error (cm)***	***Angle error (degrees)***		
			X-axis	**Y-axis**	**Z-axis**
4	120	0.74	0.34	0.04	1.37
2	120	1.41	2.54	3.05	4.51
4	156	1.31	0.72	0.43	1.79
2	156	3.13	2.28	4.34	2.63

dataset, the positioning error was twice as high for both the heights with the same overall pattern of increasing error with increase in height being observed. The angle error is also twice as high with no such overall pattern with the height from the transmitter. The full light dataset observed high errors only for the z axis angle while the partial light dataset performs similarly for all three axes with the errors remaining less than five degrees for the individual axes.

IV. CONCLUSION

A camera based VLP technique for pose and position detection from a single partially visible LED was proposed. The light location and orientation were assumed to be known and the relative position of the receiver with respect to the transmitter was obtained using a structure-based technique. The proposed technique was shown to perform better than the current SOTA solution on both the pose and positioning accuracy. The mean 3D error was shown to be less than 1cm when averaged across four different heights for fully visible lights. The proposed technique was shown to achieve sub six cm accuracy when only two corners of the LED were visible at two different heights from the transmitter. This can be used to address outages in indoor positioning increasing the robustness of indoor navigation solution. A more general solution encompassing different light shapes and trajectories of motion along with the extent to which partially visible lights can be used for VLP will be further explored.

ACKNOWLEDGMENT

This Research is supported by the RIE2020 Industry Alignment Fund - Industry Collaboration Projects Funding Initiative (Award No. I1801E0020) administered by the Agency for Science, Technology and Research (A*STAR), as well as cash and in-kind contribution from Surbana Jurong Pte Ltd.

REFERENCES

[1] J. Torres-Sospedra, D. P. Q. Gaibor, J. Nurmi, Y. Koucheryavy, E. S. Lohan, and J. Huerta, "Scalable and efficient clustering for fingerprint-based positioning," *IEEE Internet of Things Journal*, vol. 10, no. 4, pp. 3484–3499, feb 2023.

[2] S. C. Narasimman and A. Alphones, "Dumbloc: Dumb indoor localization framework using wifi fingerprinting," *IEEE Sensors Journal*, pp. 1–1, 2024.

[3] W. Shao, H. Luo, F. Zhao, Y. Ma, Z. Zhao, and A. Crivello, "Indoor positioning based on fingerprint-image and deep learning," *IEEE Access*, vol. 6, pp. 74 699–74 712, 2018.

[4] L. Kanaris, A. Kokkinis, A. Liotta, and S. Stavrou, "Combining smart lighting and radio fingerprinting for improved indoor localization," in *2017 IEEE 14th International Conference on Networking, Sensing and Control (ICNSC)*. IEEE, may 2017.

[5] Z. Zhu, Y. Yang, M. Chen, C. Guo, and Y. Bai, "Visible light positioning based on a single luminaire: A novel visual odometry assisted algorithm," in *ICC 2023 - IEEE International Conference on Communications*. IEEE, May 2023.

[6] R. Zhang, W.-D. Zhong, Q. Kemao, and S. Zhang, "A single LED positioning system based on circle projection," *IEEE Photonics Journal*, vol. 9, no. 4, pp. 1–9, aug 2017.

[7] L. Bai, Y. Yang, M. Chen, C. Feng, C. Guo, W. Saad, and S. Cui, "Computer vision-based localization with visible light communications," *IEEE Transactions on Wireless Communications*, vol. 21, no. 3, pp. 2051–2065, mar 2022.

[8] H. Cheng, C. Xiao, Y. Ji, J. Ni, and T. Wang, "A single led visible light positioning system based on geometric features and cmos camera," *IEEE Photonics Technology Letters*, vol. 32, no. 17, pp. 1097–1100, Sep. 2020.

[9] J. Hao, J. Chen, and R. Wang, "Visible light positioning using a single led luminaire," *IEEE Photonics Journal*, vol. 11, no. 5, pp. 1–13, Oct. 2019.

[10] B. Hussain, Y. Wang, R. Chen, and C. P. Yue, "Camera pose estimation using a vlc-modulated single rectangular led for indoor positioning," *IEEE Transactions on Instrumentation and Measurement*, vol. 71, pp. 1–11, 2022.

[11] S. C. Narasimman and A. Alphones, "Tree-based single led indoor visible light positioning technique," in *TENCON 2023 - 2023 IEEE Region 10 Conference (TENCON)*. IEEE, Oct. 2023.

[12] L. Hua, Y. Zhuang, and J. Yang, "Deep learning-based fusion of visible light positioning and IMU sensors," in *2021 20th International Conference on Ubiquitous Computing and Communications (IUCC/CIT/DSCI/SmartCNS)*. IEEE, dec 2021.

[13] C. Qin and X. Zhan, "VLIP: Tightly coupled visible-light/inertial positioning system to cope with intermittent outage," *IEEE Photonics Technology Letters*, vol. 31, no. 2, pp. 129–132, jan 2019.

[14] J. Shi and Tomasi, "Good features to track," in *Proceedings of IEEE Conference on Computer Vision and Pattern Recognition CVPR-94*. IEEE Comput. Soc. Press, 1994.

[15] Y.-S. Kuo, P. Pannuto, K.-J. Hsiao, and P. Dutta, "Luxapose," in *Proceedings of the 20th annual international conference on Mobile computing and networking*. ACM, sep 2014.